

# Infrared and Ultraviolet Absorptions of Matrix Isolated C<sub>6</sub>O<sub>2</sub>

Dmitry Strelnikov,<sup>†</sup> Roman Reusch, and Wolfgang Krätschmer\*

Max-Planck-Institut für Kernphysik, Heidelberg, Germany

Received: June 13, 2006; In Final Form: September 7, 2006

In the course of our research into carbon chains trapped in matrices of molecular oxygen, we encountered an IR absorption line at 2180.4 cm<sup>-1</sup>, which we tentatively assigned to linear C<sub>6</sub>O<sub>2</sub>.<sup>1</sup> In this article, we describe our attempts to confirm the assignment by partial isotopic substitution of carbon by <sup>13</sup>C and oxygen by <sup>18</sup>O. A detailed analysis of the IR vibration pattern allowed the unambiguous identification of the carrier of the IR absorption as C<sub>6</sub>O<sub>2</sub>. The identification work was very much facilitated by the observation that it is possible to produce and destroy C<sub>6</sub>O<sub>2</sub> in a controlled fashion by suitable laser exposures. With the help of this feature, most of the confusing spectral background could be removed. Two infrared absorptions at 2180.4 (ν<sub>5</sub>) and 1817.7 cm<sup>-1</sup> (ν<sub>6</sub>) and ultraviolet absorption at 252 nm were assigned to the C<sub>6</sub>O<sub>2</sub> molecule—all figures are valid for oxygen matrices. The obtained spectral data are compared with results of quantum chemical calculations. DFT B3LYP/6-31G(d) and semiempirical PM3 methods were used for geometry optimization and calculation of vibrational frequencies. CIS and TD-DFT were used to calculate the electronic absorption spectrum.

## 1. Introduction

The oxides of carbon molecules play a role in various fields of research, for example, in atmospheric science, in combustion, and, since carbon and oxygen have similar cosmic abundances, also in cometary, stellar, and interstellar chemistry.<sup>2–10</sup> Measurements of IR and UV–vis spectra of C<sub>n</sub>O<sub>m</sub> allow an improved understanding the nature of these oxides and shed some light on the processes in which they are involved.

Many of the observed IR absorptions of carbon oxides belong to linear species (except CO<sub>3</sub>) in which the molecular backbone is a carbon chain C<sub>n</sub>. Considerations based on molecular orbital (MO) theory and quantum chemical calculations suggest that, similar to naked carbon chains, oxides of carbon chains have a singlet ground state if they contain an odd number of carbon atoms and a triplet ground state in the case of an even number of carbons.<sup>11</sup> For oxides with an odd number of carbon atoms, the IR absorptions of CO, CO<sub>2</sub>, CO<sub>3</sub>,<sup>12</sup> C<sub>3</sub>O,<sup>13–15</sup> C<sub>3</sub>O<sub>2</sub>,<sup>16</sup> C<sub>5</sub>O<sub>2</sub>,<sup>17,18</sup> and C<sub>7</sub>O<sub>2</sub><sup>19</sup> are known. Likewise, for species with even number of carbon atoms, information about IR absorptions of C<sub>2</sub>O,<sup>20</sup> C<sub>4</sub>O,<sup>17</sup> C<sub>4</sub>O<sub>2</sub>,<sup>21</sup> and C<sub>6</sub>O<sup>19</sup> exists in the literature.<sup>22</sup> Furthermore, some IR absorptions have tentatively been assigned to C<sub>5</sub>O, C<sub>7</sub>O, and C<sub>9</sub>O.<sup>23</sup> Different oxides of carbon chains can be produced chemically from organic precursors. This was achieved even for such a long species as C<sub>7</sub>O<sub>2</sub>.<sup>19</sup> There has also been an unsuccessful attempt reported to synthesize C<sub>6</sub>O<sub>2</sub> by pyrolysis of dicarbonic acid chloride and dimethylester.<sup>24</sup> Some of the oxides, for example, C<sub>5</sub>O, C<sub>7</sub>O, and C<sub>9</sub>O, could not be produced by the usual chemical techniques. In such cases, the use of carbon-rich cryogenic matrices, also containing some additional molecules with oxygen atoms, turned out to be helpful. An example of such an approach is the experiment where Ar matrices containing C<sub>n</sub> and H<sub>2</sub>O molecules were subjected to UV irradiation.<sup>23</sup> In our experiments, we used C<sub>n</sub> species of carbon vapor trapped either in pure oxygen matrices

or in matrices consisting of mixtures of oxygen and argon. Upon matrix deposition, free oxygen atoms form, probably by the reaction of atomic carbon with molecular oxygen (noticeable by the appearance of O<sub>3</sub> absorptions in the spectra). Simultaneously, several carbon oxides C<sub>n</sub>O<sub>m</sub> are spontaneously produced.<sup>25</sup>

Concerning spectroscopic techniques for the characterization of carbon oxides, UV–vis and IR absorption spectroscopy provide a lot of information about these molecules. Laser diode infrared spectroscopy was used for species which could be prepared in the gas phase (CO, CO<sub>2</sub>, C<sub>3</sub>O, C<sub>2</sub>O, C<sub>3</sub>O<sub>2</sub>, C<sub>5</sub>O<sub>2</sub>). In cases where the molecules of interest could not be prepared in sufficient amounts in the gas phase, FTIR measurements were carried out on matrices (CO<sub>3</sub>, C<sub>4</sub>O, C<sub>4</sub>O<sub>2</sub>, C<sub>5</sub>O, C<sub>6</sub>O, C<sub>7</sub>O, C<sub>7</sub>O<sub>2</sub>, C<sub>9</sub>O). Much less is known about the electronic transitions of carbon oxides. With the exception of the well-studied molecules CO, CO<sub>2</sub>, and C<sub>2</sub>O, the UV–vis absorptions of just a few species, namely, C<sub>4</sub>O<sub>2</sub>, C<sub>5</sub>O<sub>2</sub>, and C<sub>7</sub>O<sub>2</sub>, were measured in argon matrices. Nothing is known about the vibrational and electronic transitions of the other carbon oxides.

In a previous investigation of carbon chains trapped in cryogenic oxygen matrices, we encountered IR absorption at 2180.4 cm<sup>-1</sup>, which we tentatively assigned to linear C<sub>6</sub>O<sub>2</sub>.<sup>1</sup> In this article, we confirm our previous finding and report on measurements of the IR lines and electronic absorption features of this molecule.

## 2. Approach

The exposure of O<sub>2</sub>-matrix-isolated carbon and carbon oxide C<sub>n</sub>O<sub>m</sub> species to laser radiation at certain wavelengths in the UV–vis leads to selective destruction of molecules, which can be observed as a correlated decrease of UV–vis and IR absorptions.<sup>1,25</sup> We furthermore found that by laser exposure we cannot only destroy but also selectively produce some of the molecules. One of these molecules is the species considered here. To identify the carrier, we used the partial isotopic substitution of carbon by <sup>13</sup>C and oxygen by <sup>18</sup>O and made use

\* w.kraetschmer@mpi-hd.mpg.de.

† dima@mpi-hd.mpg.de.

of the fact that we could produce and destroy the molecule by a suitable laser exposure in a controlled fashion. This latter feature considerably helped to identify the isotopomeric species of the carrier in the IR and also to establish the UV–vis absorptions of  $C_6O_2$ .

### 3. Experimental Section

Our experimental setup was designed to measure the infrared and ultraviolet spectra of the same sample of matrix isolated carbon molecules. The setup has been described elsewhere.<sup>26</sup>

In brief, to produce carbon vapor, we evaporated two graphite rods (a 6-mm-diameter rod contacting a 3-mm-diameter rod) by resistive heating in a vacuum. Carbon vapor molecules (mostly C,  $C_2$ , and  $C_3$ ) were co-deposited either with pure oxygen (99.998%) or with an argon–oxygen mixture (90% Ar + 10%  $O_2$ ) on a Rh-coated sapphire substrate kept at 10–28 K. The ratio of carbon to matrix molecules was chosen to about 1:1000. Infrared and UV–vis spectra were measured by an FTIR and OMA spectrometer, respectively. The UV–vis spectra were recorded during 60 s in order to minimize the effect from UV irradiation by our deuterium lamp light source.

To deduce the number of oxygen atoms in the molecule, a mixture of 50%  $^{16}O_2$  + 50%  $^{18}O_2$  was used as a matrix material. The evaporation of a 3-mm-diameter graphite  $^{12}C$  rod stuffed with amorphous 99%  $^{13}C$  powder was performed to gain information on the number of carbon atoms in the molecule. For this purpose, holes of 1–2 mm diameter were drilled into the graphite rod and filled with  $^{13}C$  powder. To increase the concentration of  $^{13}C$  with respect to  $^{12}C$ , the part of the 3 mm graphite rod facing toward the sample substrate was polished flat.

After deposition, the matrix was exposed to the beam of a XeCl excimer pumped dye laser which was tuned to the desired wavelengths. IR and UV–vis absorption spectra (with  $0.3\text{ cm}^{-1}$ , respectively, 0.5 nm resolution) were measured before and after laser irradiation.

It turned out that an effective depletion of the absorption at  $2180.4\text{ cm}^{-1}$  can be achieved by irradiation of the sample at 308 nm (i.e., the pump beam of a XeCl excimer laser). Likewise, the same absorption can be depleted using the 450–455 nm laser wavelengths. A revival or increase of the  $2180.4\text{ cm}^{-1}$  band can be obtained by irradiating the sample at 437–440 nm. For irradiations at 450–455 nm and 437–440 nm, a dye solution of Coumarin 2 (LC4500)<sup>27</sup> was applied (average output power  $\sim 8\text{ mW}$ ).

A quadrupole mass spectrometer was used for monitoring of molecules produced in the source. All experiments were performed under high-vacuum conditions (order of  $10^{-7}$  mbar).

### 4. Results and Discussion

We carried out our experiment in such a way that information about the number of atoms in the molecule of interest could be obtained through direct counting of the isotopomeric lines in the infrared spectrum. Nevertheless, to support our assignments, we also performed quantum chemical calculations using commercially available software, *Gaussian 98*<sup>28</sup> (for DFT) and *Hyperchem 6*<sup>29</sup> (for PM3). As already mentioned in the Introduction, PM3 and DFT calculations suggest that  $C_6O_2$  has a triplet ground state. The geometry optimization and calculation of vibrational modes were done for the triplet ground state using the restricted (half-electron approximation) and unrestricted semiempirical PM3 method and with the unrestricted DFT b3lyp/6-31g(d) method. All calculations predict two intense infrared active stretching vibrations ( $\nu_5$  and  $\nu_6$ ), of which one

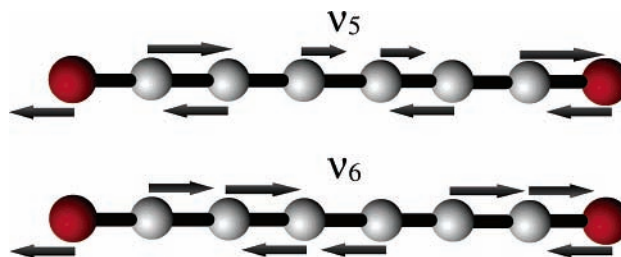


**Figure 1.** Vibrational pattern of two intense IR-active modes of  $C_6O_2$ .

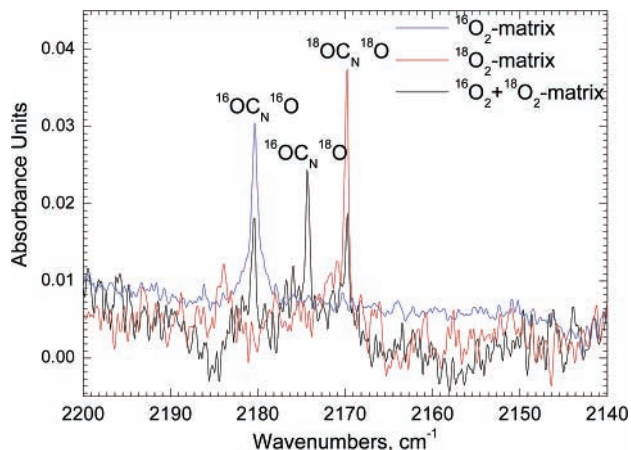


**Figure 2.** The species suspected to be  $C_6O_2$  is produced by laser exposure of carbon molecules in an  $O_2$  matrix. Shown are difference IR spectra after laser irradiation at 440 nm. The presence of three peaks at 2180.4, 2174.3, and 2169.8  $\text{cm}^{-1}$  in a mixed 50%  $^{16}O_2$  + 50%  $^{18}O_2$  matrix indicates that the carrier of that feature is a dioxide.

**TABLE 1: Unscaled Calculated Vibrational Frequencies and IR Intensities in Parentheses (in  $\text{km/mol}$ ) of Triplet  $C_6O_2$**

	rPM3, $\text{cm}^{-1}$	uPM3, $\text{cm}^{-1}$	B3LYP/6-31G(d), $\text{cm}^{-1}$
$\nu_1(\sigma_g)$	2417(0)	2455.3(0)	2396.8(0)
$\nu_2(\sigma_g)$	2270.1(0)	2291.6(0)	2141.9(0)
$\nu_3(\sigma_g)$	1595.4(0)	1596.9(0)	1486.5(0)
$\nu_4(\sigma_g)$	542.4(0)	542.8(0)	493.1(0)
$\nu_5(\pi_u)$	2376.4(4253)	2353.6(6419)	2297(4348)
$\nu_6(\pi_u)$	2058.5(86)	2055.3(256)	1885.6(257)
$\nu_7(\pi_u)$	1081.5(4)	1080.5(5)	991.8(45)
$\nu_8(\sigma_g)$	585(0)	574.2(0)	662.5(0)
$\nu_9(\sigma_g)$	479.3(0)	464.3(0)	477.8(0)
$\nu_{10}(\sigma_g)$	172.1(0)	167.5(0)	161(0)
$\nu_{11}(\pi_u)$	531.4(59)	514.2(62)	487.1(31)
$\nu_{12}(\pi_u)$	352(0)	349.1(0)	375(0)
$\nu_{13}(\pi_u)$	63.4(0)	62.1(0)	63.8(1)

( $\nu_5$ ) is extremely strong; see Table 1 and Figure 1. The ground-state geometries obtained by each method are all linear, with the following bond lengths (in ångströms): 1.1752–1.2879–1.266–1.2825–1.266–1.2879–1.1752 (restricted PM3), 1.1745–1.2858–1.267–1.28–1.267–1.2858–1.1745 (unrestricted PM3), 1.1791–1.2829–1.2855–1.2803–1.2855–1.2829–1.1791 (DFT b3lyp/6-31g(d)).

The result of the isotopic substitution of oxygen atoms in the molecule is displayed in Figure 2. From the pattern of lines, one can clearly recognize that there are two oxygen atoms contained in the species, confirming our previous measurements.<sup>1</sup>

We produced different  $^{13}C$ – $^{12}C$  isotopic mixtures of carbon to derive the number of carbon atoms. As we found by mass spectroscopy, our source produces about 45% C, 10%  $C_2$ , and 45%  $C_3$ . We further observed that the evaporation of a natural  $^{12}C$ -graphite rod filled with  $^{13}C$  amorphous carbon does not

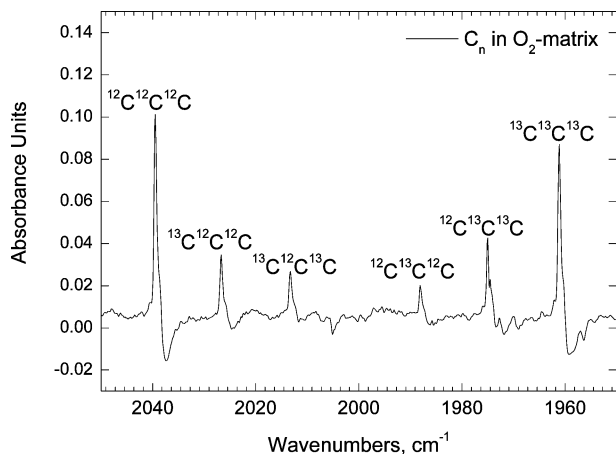


**Figure 3.** Difference spectrum of the matrix containing <sup>13</sup>C-enriched carbon molecules, after cooling from 25 K ( $\beta$ -O<sub>2</sub>) to 10 K ( $\alpha$ -O<sub>2</sub>). As result of a peculiar matrix effect, the absorption lines of C<sub>3</sub> in the  $\alpha$ -phase of oxygen are considerably narrower than in the  $\beta$ -phase and are also slightly blue-shifted. The difference spectrum thus highlights the C<sub>3</sub> isotopomers. One clearly sees that <sup>12</sup>C<sub>3</sub> and <sup>13</sup>C<sub>3</sub> are more abundant than the other isotopomers of C<sub>3</sub>.

provide a statistical mixture of carbon atoms. The distribution of isotopomers which we obtained for the C<sub>3</sub> molecule (also with the help of IR spectroscopy) can be approximated by two independent distributions of statistically mixed carbon sources, the first <sup>12</sup>C enriched by <sup>13</sup>C and the second <sup>13</sup>C enriched by <sup>12</sup>C.

As a result of such nonstatistical mixtures, we occasionally obtained samples mostly containing the pure isotopomers <sup>12</sup>C<sub>3</sub> and <sup>13</sup>C<sub>3</sub>. This can be clearly recognized in Figure 3, which shows the difference spectrum of the same matrix sample recorded at two different solid oxygen phases, namely, in the  $\alpha$ -O<sub>2</sub> phase at 10 K and the  $\beta$ -O<sub>2</sub> phase at 25 K. We noticed during our work that the absorption lines of C<sub>3</sub> have exceptional behavior: They considerably sharpen (and show a slight shift) in going from the  $\beta$  to the  $\alpha$  phase. Even though we do not understand this effect completely, we make use here of the difference in the spectra to remove background lines (which stay almost unchanged) and to obtain a clear and complete isotopomeric line pattern of C<sub>3</sub>. In one such case of isotopic replacement, we observed three strong isotopomeric absorptions in C<sub>6</sub>O<sub>2</sub> (Figure 4A). This observation suggests that a close relationship exists between C<sub>3</sub> and the two oxides C<sub>6</sub>O<sub>2</sub> and C<sub>3</sub>O in the sense that the C<sub>3</sub> species are the main building blocks of the two oxides. We can obtain good agreement with the calculated pattern of lines of isotopomers (see Table 2) if we assume that the absorptions of C<sub>6</sub>O<sub>2</sub> belong to the oxides of the three most probable isotopomeric combinations of <sup>12</sup>C<sub>3</sub> and <sup>13</sup>C<sub>3</sub>, namely, (1) O<sup>12</sup>C<sub>3</sub><sup>12</sup>C<sub>3</sub>O, (2) O<sup>12</sup>C<sub>3</sub><sup>13</sup>C<sub>3</sub>O, and (3) O<sup>13</sup>C<sub>3</sub><sup>13</sup>C<sub>3</sub>O. The relevant reactions in the matrix may go like this C<sub>3</sub> + O<sub>2</sub> → C<sub>3</sub>O + O, OC<sub>3</sub> + C<sub>3</sub>O → C<sub>6</sub>O<sub>2</sub>; or alternatively C<sub>3</sub> + C<sub>3</sub> → C<sub>6</sub>, C<sub>6</sub> + O<sub>2</sub> → C<sub>6</sub>O<sub>2</sub>. The latter reaction very certainly takes place, because we observed a decrease of C<sub>6</sub> correlated with an increase of the suspected C<sub>6</sub>O<sub>2</sub> absorption.

Another isotopic mixture which we could produce was a matrix sample in which mostly <sup>12</sup>C<sub>3</sub> and small amounts of singly substituted <sup>13</sup>C<sup>12</sup>C<sup>12</sup>C and <sup>12</sup>C<sup>13</sup>C<sup>12</sup>C were present. Combining these three C<sub>3</sub> isotopomers, we obtain four probable products: O<sup>12</sup>C<sub>3</sub><sup>12</sup>C<sub>3</sub>O, O<sup>12</sup>C<sub>3</sub><sup>13</sup>C<sup>12</sup>C<sup>12</sup>CO, O<sup>12</sup>C<sub>3</sub><sup>12</sup>C<sup>13</sup>C<sup>12</sup>CO, and O<sup>12</sup>C<sub>3</sub><sup>12</sup>C<sup>12</sup>C<sup>13</sup>CO. Indeed, in Figure 4B, we see a strong main absorption line at 2180.4 cm<sup>-1</sup> and, adjacent to the main peak, three isotopomeric lines (4), (5), and (6). Again, the measured positions coincide very well with the calculated values (Table 2).

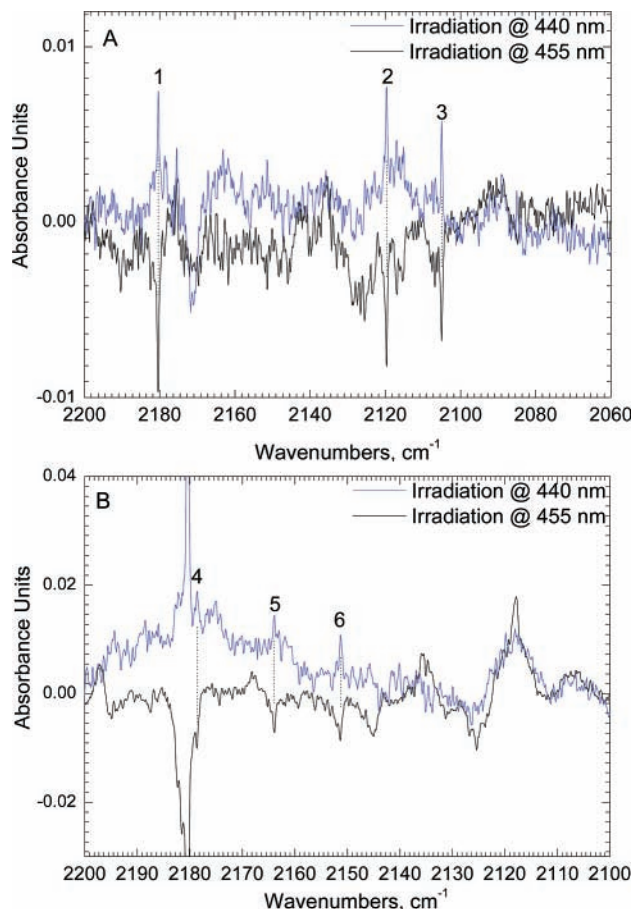


**Figure 4.** Difference IR spectra of isotopically enriched samples after laser irradiations at 440 and 455 nm. (A) The strongest isotopomeric peaks at 2180.4 (1), 2119.6 (2), and 2105 cm<sup>-1</sup> (3) belong to isotopomers <sup>12</sup>C<sub>6</sub>O<sub>2</sub>, <sup>12</sup>C<sub>3</sub><sup>13</sup>C<sub>3</sub>O<sub>2</sub>, and <sup>13</sup>C<sub>6</sub>O<sub>2</sub>, respectively. (B) The strongest isotopomeric peaks at 2178.7 (4), 2163.9 (5), and 2151.3 cm<sup>-1</sup> (6) belong to isotopomers with a singly substituted <sup>13</sup>C atom. Numbering of isotopomers here is the same as in the Table 2.

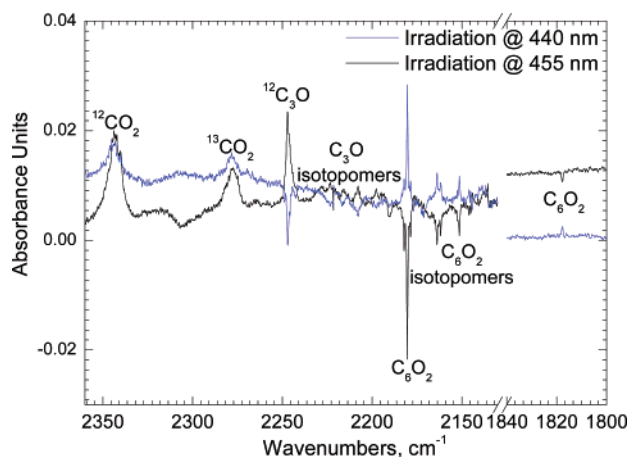


**Figure 5.** Difference IR spectra of a <sup>13</sup>C-enriched sample after laser irradiation at 440 and 455 nm. Notice the weak absorption at 1817.7 cm<sup>-1</sup> correlating with the absorption at 2180.4 cm<sup>-1</sup>. It is remarkable that the absorption of C<sub>3</sub>O anticorrelates with IR lines of C<sub>6</sub>O<sub>2</sub>.

Our assignment of the 2180.4 cm<sup>-1</sup> absorption to C<sub>6</sub>O<sub>2</sub> is also supported by the observed reversible photochemical reaction where two C<sub>3</sub>O molecules associate to form C<sub>6</sub>O<sub>2</sub>, which then can dissociate back into C<sub>3</sub>O fragments (see below). So, we conclude that the only molecule which can produce the observed distribution of isotopomeric lines is C<sub>6</sub>O<sub>2</sub>, and we assign the



**TABLE 2: IR Frequencies ( $\nu_5$ ) of Triplet  $C_6O_2$  Isotomers: Calculation and Experiment<sup>a</sup>**

	isotomer	exptl, $cm^{-1}$	rPM3, $cm^{-1}$	uPM3, $cm^{-1}$	B3LYP/6-31G(d), $cm^{-1}$
1	$O^{12}C^{12}C^{12}C^{12}C^{12}C^{12}CO$	2180.4	2180.4	2180.4	2180.4
2	$O^{12}C^{12}C^{12}C^{13}C^{13}C^{13}CO$	2119.6	2119.2	2127.8	2114.7
3	$O^{13}C^{13}C^{13}C^{13}C^{13}C^{13}CO$	2105	2104.3	2103.2	2102.9
4	$O^{12}C^{12}C^{13}C^{12}C^{12}C^{12}CO$	2178.6	2178.7	2178.6	2178.5
5	$O^{12}C^{13}C^{12}C^{12}C^{12}C^{12}CO$	2163.9	2164.8	2164.7	2161.8
6	$O^{13}C^{12}C^{12}C^{12}C^{12}C^{12}CO$	2151.3	2151.2	2162.1	2149.9

<sup>a</sup> Data are scaled to fit the main peak at  $2180.4\text{ cm}^{-1}$ . Only the data for the most probable isotomers under experimental conditions are displayed: combinations of  $^{12}C_3$  and  $^{13}C_3$  (1–3); singly  $^{13}C$  substituted  $C_6O_2$  (4–6); see text for details. The complete list of calculated frequencies can be found in the Supporting Information. Numbering of isotomers here is the same as for Figure 4.

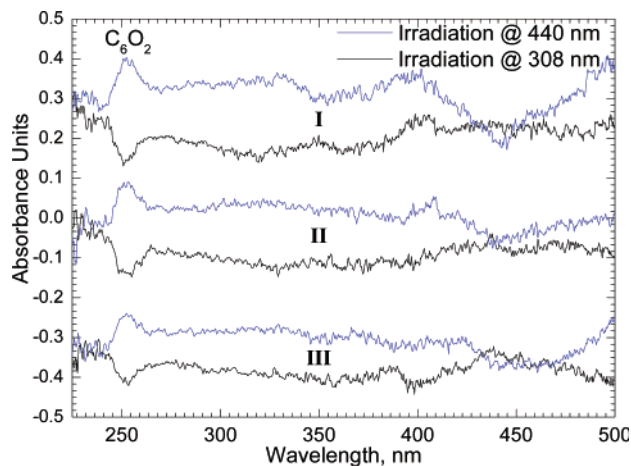
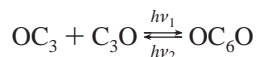


**Figure 6.** Difference UV-vis spectra after laser irradiation at 440 and 308 nm. Three consecutive creation and destruction processes of  $C_6O_2$  are shown. Absorption at 252 nm correlates with changes in the IR spectra and can therefore be assigned to  $C_6O_2$ .

strong absorption at  $2180.4\text{ cm}^{-1}$  to the antisymmetric stretching vibration  $\nu_5$ .

After subsequent laser-induced production and destruction of  $C_6O_2$ , we analyzed all changes in the IR and in the UV-vis. We found a weak absorption line at  $1817.7\text{ cm}^{-1}$ , which correlates with the absorption line at  $2180.4\text{ cm}^{-1}$  (see Figure 5). According to quantum mechanical calculations (Table 1), there is another infrared active stretching mode  $\nu_6$  of  $C_6O_2$  which has a significant intensity. Semiempirical restricted PM3 gives  $2376\text{ cm}^{-1}$  for  $\nu_5$  and 2058 or scaled value  $1889\text{ cm}^{-1}$  for  $\nu_6$  ( $\nu_{6\text{scaled}} = \nu_{6\text{calc}}\nu_{5\text{exp}}/\nu_{5\text{calc}}$ ). DFT (b3lyp/6-31g(d)) gives  $2297\text{ cm}^{-1}$  for  $\nu_5$  and 1886 or scaled  $1791\text{ cm}^{-1}$  for  $\nu_6$ . The experimental value  $1817.7\text{ cm}^{-1}$  is between calculated PM3 and DFT values. We assign the absorption at  $1817.7\text{ cm}^{-1}$  as the  $\nu_6$  IR-active vibrational stretching mode of  $C_6O_2$ .

Another finding is the observed anticorrelation of the  $C_3O$  and the  $C_6O_2$  IR absorption upon laser irradiation (Figure 5). This suggests a following reversible reaction



Since the molecules are trapped in the matrix,  $C_3O$  molecules remain in close vicinity even after  $C_6O_2$  dissociation. The laser at 440 nm seems to excite  $C_3O$ , leading to a reassociation of the two  $C_3O$  molecules.

In the UV-vis domain, the only absorption which we found correlating with the IR absorption at  $2180.4\text{ cm}^{-1}$  is the absorption feature centered at 252 nm with a half-width of about 15 nm (see Figure 6).

To compare our UV-vis absorption data with theory, singly excited configuration interaction (CIS<sup>29</sup>) and time-dependent density functional theory (TD-DFT<sup>28</sup>) calculations were carried

**TABLE 3: Electronic Absorptions of  $C_6O_2$ , Calculated Using the CIS Method<sup>a</sup>**

UV-vis absorption nm	oscillator strength
602.2	0.0215
267.9	1.5774
247.6	1.8083
195.5	0.0221
180.6	0.2892
164.2	0.5519
156.1	0.6080
147.0	0.0653
146.7	0.0103
141.9	0.0151

<sup>a</sup> Only absorptions with oscillator strengths greater than  $10^{-2}$  and with wavelengths greater than 140 nm are displayed.

**TABLE 4: Electronic Absorptions of  $C_6O_2$ , Calculated Using the TD-DFT B3LYP/6-31G(d) Method<sup>a</sup>**

UV-vis absorption nm	oscillator strength
429.1	0.0202
212.2	3.382
168.0	0.145
142.4	0.034

<sup>a</sup> Only absorptions with oscillator strengths greater than  $10^{-2}$  are displayed.

out. CIS performed for  $C_6O_2$  (triplet, optimized by restricted PM3) included configurations with an excitation energy of less than 20 eV. The calculation predicts two intense electronic absorptions at 247 and 268 nm in the UV-vis region. (Table 3). The TD-DFT method with the B3LYP/6-31g(d) functional and basis set yielded among the first 50 excited triplet states only one strong absorption in the UV-vis at 212 nm (Table 4).

The CIS and TD-DFT calculations predict intense absorptions in the range between 210 and 270 nm and thus are in qualitative agreement with our observations. For comparison of experimental and theoretical results, it should be considered that our data are affected by matrix broadening and shifts.

The fact that laser irradiations at 308 and 450–455 nm lead to dissociation of  $C_6O_2$  may indicate the presence of weak electronic absorptions at these wavelengths. Our CIS and TD-DFT calculations also predict some small absorptions at wavelengths longer than 350 nm. However, it is only possible to achieve qualitative correspondence between numerical results and observations at these levels of theory. The excitation of  $C_6O_2$  at 308 nm could also originate from two-photon absorption process, as at this wavelength, irradiation was made directly by a powerful XeCl excimer laser.

## 5. Conclusion

Using laser-induced photochemical reactions in cryogenic oxygen matrices containing carbon molecules, we assigned two infrared absorptions at  $2180.4\text{ cm}^{-1}$  ( $\nu_5$ ) and  $1817.7\text{ cm}^{-1}$  ( $\nu_6$ ) and ultraviolet absorption at 252 nm to the  $C_6O_2$  molecule. We found

that C<sub>6</sub>O<sub>2</sub> can be formed photochemically from C<sub>3</sub>O and that the reverse process, namely, the photochemical dissociation of C<sub>6</sub>O<sub>2</sub> into C<sub>3</sub>O, can also be obtained. Our isotopic replacement experiments suggest that C<sub>3</sub> is the building unit from which the oxides C<sub>3</sub>O and C<sub>6</sub>O<sub>2</sub> originate.

**Acknowledgment.** We thank Ruth Alberts for technical assistance and the Max-Planck-Society for continuous financial support.

**Supporting Information Available:** The complete list of calculated  $\nu_5$  vibrational frequencies for all isotopomers of C<sub>6</sub>O<sub>2</sub> is displayed in Table S1. This material is available free of charge via the Internet at <http://pubs.acs.org>.

## References and Notes

- (1) Strelnikov, D. Selective Laser-Induced Oxidation of Carbon Chain Molecules in Cryogenic Matrices. Ph.D. Thesis, 2004; <http://www.ub.uni-heidelberg.de/archiv/5230>.
- (2) Smith, A. M.; Stecher, T. P. *Astrophys. J.* **1971**, *164*, L43–L47.
- (3) Matthews, H. E.; Irvine, W. M.; Friberg, P.; Brown, R. D.; Godfrey, P. D. *Nature (London)* **1984**, *310* (5973), 125–126.
- (4) Ohishi, M.; Ishikawa, S.-I.; Yamada, C.; Kanamori, H.; Irvine, W. M.; Brown, R. D.; Godfrey, P. D.; Kaifu, N.; Suzuki, H. *Astrophys. J.* **1985**, *290*, 65–66.
- (5) Douglas, A. *Nature (London)* **1977**, *269*, 130–132.
- (6) Douglas, A. *Nat. Res. Council* **1951**, *2503*, 466–468.
- (7) Herbig, G. *Annu. Rev. Astron. Astrophys.* **1995**, *33*, 359.
- (8) Gredel, R.; van Dishoeck, E.; Black, J. *Astrophys. J.* **1989**, *338*, 1047–1070.
- (9) Lambert, D.; Sheffer, Y.; Federman, S. *Astrophys. J.* **1995**, *438*, 740–749.
- (10) Wallerstein, G.; Knapp, G. *Annu. Rev. Astron. Astrophys.* **1998**, *36*, 369–433.
- (11) Janoschek, R. *Sulfur Rep.* **1999**, *21*, 373–400.
- (12) Weissberger, E.; Breckenridge, W. H.; Taube, H. *J. Chem. Phys.* **1967**, *47*, 1764–1769.
- (13) DeKock, R. L.; Weltner, W., Jr. *J. Am. Chem. Soc.* **1971**, *93*, 7106.
- (14) Brown, R. D.; Pullin, D. E.; Rice, E. H. N.; Rodler, M. *J. Am. Chem. Soc.* **1985**, *107*, 7877.
- (15) Botschwina, P.; Reisenauer, H. P. *Chem. Phys. Lett.* **1991**, *183*, 217–222.
- (16) Shimanouchi, T. *J. Phys. Chem. Ref. Data* **1977**, *6* (3), 993–1102.
- (17) Maier, G.; Reisenauer, H. P.; Schäfer, U.; Balli, H. *Angew. Chem.* **1988**, *100* (4), 590–592.
- (18) Holland, F.; Winnewisser, M.; Maier, G.; Reisenauer, H. P.; Ulrich, A. *J. Mol. Spectrosc.* **1988**, *130*, 470–474.
- (19) Maier, G.; Reisenauer, H. P.; Ulrich, A. *Tetrahedron Lett.* **1991**, *32* (35), 4469–4472.
- (20) Jacox, M. E.; Milligan, D. E.; Moll, N. G.; Thompson, W. E. *J. Chem. Phys.* **1965**, *43* (10), 3734–3746.
- (21) Maier, G.; Reisenauer, H. P.; Balli, H.; Brandt, W.; Janoschek, R. *Angew. Chem.* **1990**, *102* (8), 920–925.
- (22) *NIST Chemistry WebBook*; National Institute of Science and Technology; <http://webbook.nist.gov>.
- (23) Dibben, M.; Szczepanski, J.; Wehlburg, C.; Vala, M. *J. Chem. Phys.* **2000**, *104*, 3584–3592.
- (24) Ruppel, R. Neue Heterokumulene und Carbene. Ph.D. Thesis (in German), 1999; <http://geb.uni-giessen.de/geb/volltexte/1999/76>.
- (25) Strelnikov, D.; Reusch, R.; Krätschmer, W. *J. Phys. Chem. A* **2005**, *109* (34), 7708–7713.
- (26) Cermak, I.; Monninger, G.; Krätschmer, W. *Adv. Mol. Struct. Res.* **1997**, *3*, 117–146.
- (27) Brackmann, U. *Lambdachrome Laser Dyes Data Sheets*; Lambda Physik GmbH, D-37079 Göttingen, Germany; 1994.
- (28) Frisch, M. J.; Trucks, G. W.; Schlegel, H. B.; Scuseria, G. E.; Robb, M. A.; Cheeseman, J. R.; Zakrzewski, V. G.; Montgomery, J. A., Jr.; Stratmann, R. E.; Burant, J. C.; Dapprich, S.; Millam, J. M.; Daniels, A. D.; Kudin, K. N.; Strain, M. C.; Farkas, O.; Tomasi, J.; Barone, V.; Cossi, M.; Cammi, R.; Mennucci, B.; Pomelli, C.; Adamo, C.; Clifford, S.; Ochterski, J.; Petersson, G. A.; Ayala, P. Y.; Cui, Q.; Morokuma, K.; Malick, D. K.; Rabuck, A. D.; Raghavachari, K.; Foresman, J. B.; Cioslowski, J.; Ortiz, J. V.; Stefanov, B. B.; Liu, G.; Liashenko, A.; Piskorz, P.; Komaromi, I.; Gomperts, R.; Martin, R. L.; Fox, D. J.; Keith, T.; Al-Laham, M. A.; Peng, C. Y.; Nanayakkara, A.; Gonzalez, C.; Challacombe, M.; Gill, P. M. W.; Johnson, B. G.; Chen, W.; Wong, M. W.; Andres, J. L.; Head-Gordon, M.; Replogle, E. S.; Pople, J. A. *Gaussian 98*, revision A.9; Gaussian, Inc.: Pittsburgh, PA, 1998.
- (29) *Hyperchem for Windows*, release 6.02.; Hypercube, Inc., Gainesville, Florida, 1999.